Journal of Science and Technology ‒ Smart Systems and Devices
Volume x, Issue x, Month Year, ppp–ppp

Thermo-Hydraulic Evaluation of a Diamond-Baffled Parallel-Channel Cold Plate Using CFD and Grey Relational Analysis

Duong Do Trong[1], Hoang Trinh Minh[1], Hoan Vu Dinh[1], Hieu Ha Van[2,*], Dung Nguyen Tien[1], Viet Le Bao[1]
[1]School of Mechanical Engineering, Hanoi University of Science and Technology, Ha Noi, Vietnam
[2]Faculty of Motive Power Engineering, University of Transport Technology, Ha Noi, Vietnam
[*]Corresponding author email:hieuhv@utt.edu.vn

Abstract

Liquid-cooled cold plates have been widely adopted in battery thermal management systems owing to their superior heat removal capability. This study systematically investigates the thermo-hydraulic performance of a parallel-flow cold plate incorporating diamond baffles using three-dimensional computational fluid dynamics. A parametric investigation involving 70 geometric configurations was conducted by varying the diagonal length and baffle height. The effects of these geometric parameters on the maximum temperature, temperature difference, and pressure drop were analyzed, followed by a Grey Relational Analysis-based multi-objective evaluation to identify the best-performing configuration under the adopted equal-weight GRA scheme. The results indicate that the configuration with d = 9.49 mm and h = 8 mm achieved the highest grey relational grade of 0.868. At the reference operating condition of 0.06 kg/s, this configuration reduced the maximum temperature by 19.83 K and the temperature difference by 17.62 K, while increasing the pressure drop by 560.07 Pa (5.01 times the baseline value). The present study provides practical design guidance for diamond-baffle parallel-flow cold plates and demonstrates the effectiveness of combining CFD with GRA for thermo-hydraulic evaluation in battery thermal management systems.

Keywords: Battery thermal management system, computational fluid dynamics, diamond baffle, grey relational analysis, parallel-flow cold plate, thermo-hydraulic performance.

1. Introduction

The rapid development of electric vehicles (EVs) has driven the widespread adoption of lithium-ion batteries because of their high energy density and long cycle life. However, battery performance, lifespan, and safety are highly sensitive to operating temperature. Therefore, an efficient battery thermal management system (BTMS) is essential to maintain batteries within the recommended temperature range and ensure temperature uniformity. Among the available cooling technologies, liquid cooling is widely recognized as one of the most effective solutions due to its superior heat removal capability and thermal management performance [1-3].

To improve the cooling performance of liquid-cooled BTMS, various passive flow-enhancement structures, such as ribs, pin fins, cylindrical obstacles, and baffles, have been incorporated into cold plates [4, 5-7]. These structures enhance heat transfer by promoting coolant mixing and disrupting the thermal boundary layer, but inevitably increase hydraulic resistance [4, 6]. Among these passive enhancement structures, diamond-shaped baffles are of particular interest because their geometry can locally accelerate the coolant, promote fluid mixing, and periodically disturb the thermal boundary layer, while potentially mitigating the excessive pressure loss associated with conventional bluff-body obstacles. Therefore, they represent a promising candidate for improving the thermo-hydraulic performance of liquid-cooled battery cold plates.

Despite the studies on flow-enhancement structures, investigations of diamond-baffle configurations for parallel-flow cold plates remain relatively limited. In particular, the combined effects of baffle diagonal length and height have received relatively limited attention. Furthermore, previous studies have often evaluated cooling performance using individual thermal or hydraulic indicators [5, 6], whereas integrated evaluations considering multiple thermo-hydraulic objectives remain relatively limited [8].

Motivated by these research gaps, this study systematically investigates a parallel-flow cold plate equipped with diamond-shaped baffles using three-dimensional computational fluid dynamics (CFD). The effects of baffle diagonal length and height on the thermo-hydraulic characteristics are first analyzed, followed by a Grey Relational Analysis (GRA)-based multi-objective evaluation to identify the optimal configuration. The main contributions of this study are twofold: (i) systematically investigating the thermo-hydraulic effects of diamond-shaped baffles with different diagonal lengths and heights and evaluating the performance of the resulting configurations in a parallel-flow liquid-cooled cold plate; and (ii) applying GRA to identify the best-performing diamond-baffle configuration by

p-ISSN 3093-3285
e-ISSN 3093-3315
https://doi.org/10.51316/jst.xxx.ssad.xxxx.xx.x.x
Received: Jul 22, 2026; Revised: Aug 25, 2026;
Accepted: Sep 3, 2026; Online: Sep 8, 2026

simultaneously considering maximum temperature, temperature difference, and pressure drop.

2. Model Development

2.1. Physical Model

In this study, a baseline configuration and an enhanced configuration of a battery cold plate for BTMS were proposed and investigated, as illustrated in Fig. 1. The system consists of a cold plate with a height H = 12 mm located beneath the battery module. The internal structure of the cold plate comprises seven parallel flow channels. The coolant flows from the inlet to the outlet, both having dimensions: Hin x Win = Hout x Wout = 10 mm × 10 mm, through straight and continuous channels.

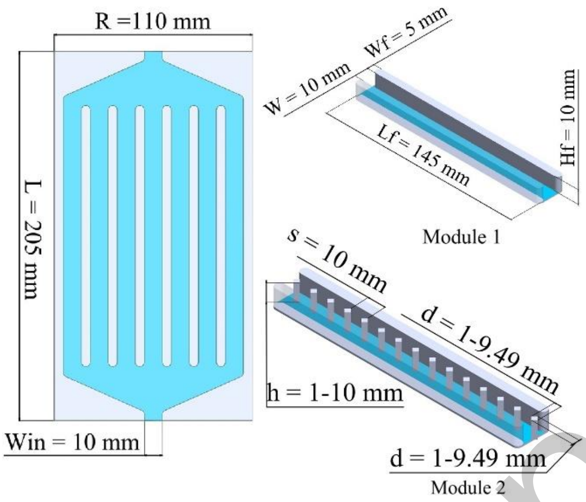

Fig. 1. Baseline and enhanced cold plate configurations

Table 1. Geometric parameters of the configurations

Symbol	Description	Dimension (mm)
L	Length of the cold plate	205
R	Width of the cold plate	110
H	Height of the cold plate	12
Hin/Hout	Inlet/Outlet height	10
Win/Wout	Inlet/Outlet width	10
Lf	Flow distributor length	145
Wf	Flow distributor width	5
W	Width of mini channel	10
Hf	Flow distributor height	10
d	The diagonal length of baffle	1-9.49
h	Baffle height	1-10
s	Baffle spacing	10

To enhance the heat transfer performance, diamond baffles were introduced into the flow channels to generate local flow disturbances, promote coolant mixing, and disrupt the thermal boundary layer. The geometric parameters of the proposed configurations are summarized in Table 1. The cold plate was assumed to be fabricated from aluminum, while water was selected as the working coolant. The coolant entered the cold plate at 293 K through the inlet and exited through the outlet. The thermophysical properties and key specifications of both the cold plate and the coolant are summarized in Table 2. For consistency throughout the study, the baseline configuration is referred to as Module 1, whereas the enhanced configuration is designated as Module 2.

Table 2. Material properties of the model

Material	Aluminum	Copper	Water
Density $[\mathrm{kg/m^3}]$	2719	8978	998.2
Specific Heat [J/(kg.K)]	871	381	4182
Thermal Conductivity [W/(m.K)]	202.4	387.6	0.6

2.2. Boundary Conditions

A three-dimensional conjugate heat transfer (CHT) model was developed to investigate the thermo-hydraulic characteristics of the BTMS. The following assumptions were adopted: (i) the coolant was assumed to be an incompressible Newtonian fluid; (ii) cases with the Reynolds number (Re) < 2300 were modeled as laminar flow, whereas cases with Re ≥ 2300 employed the SST model with correlation-based near-wall treatment; for turbulent cases, the inlet turbulence intensity and turbulent viscosity ratio were set to 5% and 10%, respectively; (iii) the no-slip boundary condition was imposed at all solid–fluid interfaces; and (iv) gravity, thermal radiation, and viscous dissipation were neglected, while fluid viscosity was retained to accurately predict pressure drop. The thermophysical properties of the coolant and solid were assumed constant.

Based on the aforementioned assumptions, the numerical model was established by solving the governing equations, including the continuity equation, the Navier–Stokes momentum equations, and the energy equation in the fluid domain, coupled with the steady-state heat conduction equation in the solid domain. These equations were solved simultaneously in their steady-state form using the finite volume method implemented in ANSYS Fluent 2024 R2. The thermo-hydraulic boundary conditions were: (i) uniform inlet velocity with a coolant temperature of 293 K; (ii) atmospheric pressure at the outlet; (iii) conjugate heat transfer at the fluid–solid interface; and (iv) a uniform heat flux of 20,000 W/m² applied to the heat-transfer surface, while the remaining walls were treated as adiabatic. The thermophysical properties of the coolant and solid were assumed constant. The uniform heat-flux condition was adopted to provide a controlled and consistent basis for comparing the investigated cold-plate configurations.

2.3. Performance Evaluation

To evaluate the thermo-hydraulic performance of the proposed cold plate configurations, GRA was employed for multi-objective optimization. GRA was selected because it enables multiple performance indicators with different physical meanings to be integrated into a single evaluation index, facilitating the quantitative comparison of different design configurations. Three performance indicators were considered: the maximum temperature ($T_{\max}$), temperature difference (ΔT), and pressure drop (ΔP) defined as:

$$\Delta T = T_{max} - T_{min};\ \Delta P = P_{in} - P_{out} \tag{1}$$

where P_{in} and P_{out} are the area-averaged static pressures at the inlet and outlet. Since lower values indicate better thermal and hydraulic performance, the smaller-the-better criterion was adopted for normalization. To reduce the sensitivity of pressure-drop normalization to its highly skewed distribution, ΔP was logarithmically transformed as $\Delta P' = \log_{10} \Delta P$ before normalization. The normalized value of each performance indicator is calculated as:

$$N_i(k) = \frac{max\big(I_i(k)\big) - I_i(k)}{max\big(I_i(k)\big) - min\big(I_i(k)\big)} \tag{2}$$

where $I_i(k)$ represents the original value of the k performance indicator for the i design configuration, while $N_i(k)$ denotes the corresponding normalized value. The normalized values range from 0 to 1, where a value closer to 1 indicates better performance. The deviation sequence between the normalized value and the reference sequence is determined by:

$$\Delta_{0i}(k) = |N_0(k) - N_i(k)| \tag{3}$$

where $N_0(k)$is the reference sequence corresponding to the ideal normalized value and is equal to 1. The maximum and minimum deviation sequences are respectively defined as:

$$\Delta_{max} = max_i \cdot max_k\big(\Delta_{0i}(k)\big) \tag{4}$$

$$\Delta_{min} = min_i \cdot min_k\big(\Delta_{0i}(k)\big) \tag{5}$$

Based on the deviation sequences, the Grey Relational Coefficient (GRC) is calculated as:

$$G_i(k) = \frac{\Delta_{min} + C \cdot \Delta_{max}}{\Delta_{0i}(k) + C \cdot \Delta_{max}} \tag{6}$$

where C is the distinguishing coefficient and was set to 0.5 in the present study. The value of C controls the distinguishing ability of the Grey Relational Coefficient and is independent of the weighting factors assigned to the performance indicators. Finally, the overall performance of each cold plate configuration is evaluated using the Grey Relational Grade (GRG), which is obtained by averaging the Grey Relational Coefficients of all performance indicators:

$$GRG_i = \sum_{k=1}^{m} W_k \cdot G_i(k) \tag{7}$$

where m is the total number of performance indicators, W_k is the weighting factor assigned to the k-th performance indicator, and $\sum_{k=1}^{m} W_k = 1$. In the present study, m = 3, corresponding to $T_{\max}$, ΔT, ΔP Equal weighting factors ($W_1 = W_2 = W_3 = 1/3$) were adopted because the objective of this study is to simultaneously evaluate thermal safety, temperature uniformity, and hydraulic performance without prioritizing any single criterion. To assess the sensitivity of the GRA ranking to the weighting scheme, three weighting sets were considered: (0.33,0.33,0.33); (0.4,0.4,0.2); (0.2,0.2,0.6) corresponding to $T_{\max}$, ΔT, ΔP. The results indicate that the best-performing configuration depends on the adopted weighting scheme, which can be adjusted according to the design priorities.

The Reynolds number (Re) was used to characterize the flow regime and was calculated based on the nominal average mass flow rate through each channel, following the formulation adopted from the reference study:

$$Re = \frac{m_{channel} \cdot D}{A \cdot \mu_L} \tag{8}$$

where $m_{channel}$ is the nominal average mass flow rate through each channel, D is the hydraulic diameter, A is the effective cross-sectional flow area, and μ_L is the dynamic viscosity of the coolant. The effective flow area was evaluated on a cross-sectional plane perpendicular to the flow direction at the baffle location, accounting for the solid areas occupied by the internal baffles.

3. Meshing Method

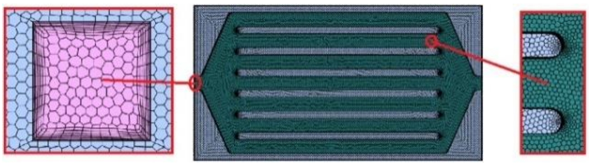

Fig. 2. Computational mesh of Module 1

A meshing strategy aimed at achieving an appropriate balance between numerical accuracy and computational cost was adopted from the numerical framework established by T. Dung Nguyen *et al.* [7]. The baseline geometry of Module 1 and the mesh-selection procedure were inherited from this previously established numerical framework to maintain consistency. In this approach, the computational domains of the cold-plate configurations were discretized using an unstructured Poly-Hexcore mesh, providing adequate spatial resolution while limiting the total number of cells and associated computational cost.

Local mesh refinement was applied at the solid–fluid interfaces, channel walls, and particularly the baffle surfaces, where large velocity and temperature gradients, as well as local flow separation and recirculation, may occur. Eight inflation layers were generated near the solid walls to adequately resolve the hydrodynamic and thermal boundary layers, thereby improving the accuracy of the near-wall thermo-hydraulic characteristics. The SIMPLE algorithm was employed for pressure–velocity coupling, with convergence criteria of 10−6 for continuity and 10−7 for the momentum and energy equations. The adopted meshing strategy was applied to Module 1, as illustrated in Fig. 2, and its mesh independence was assessed using the established mesh-selection procedure. The corresponding grid-independence results are presented in Fig. 3, demonstrating the adequacy of the selected mesh for the adopted numerical framework. The same meshing strategy was subsequently applied consistently to the diamond-baffle configurations, with local refinement maintained at the baffle surfaces to account for their geometric features and associated local flow and thermal gradients.

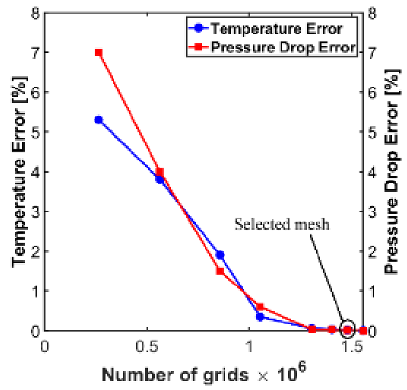

Fig. 3. Mesh independence of Module 1 [7]

Table 3. Validation results for the MMCHS model

	Mass Flow (kg/s)	Experimental Data [9]	Numerical Results [7]	Error (%)
Average Nusselt (Nu)	0.0021	4.23	4.54	7.39
	0.0027	4.62	4.81	4.04
	0.0033	4.90	5.02	2.43
	0.0039	5.08	5.50	8.29
	0.0045	5.23	5.64	7.86
Pressure drop ΔP (Pa)	0.0021	100	91.48	8.52
	0.0027	136	125.15	7.98
	0.0033	184	171.94	6.55
	0.0039	229	224.57	1.94
	0.0045	291	282.52	2.91

To assess the reliability of the numerical methodology, a benchmark study was conducted using the experimentally validated rectangular multi-mini-channel heat sink (MMCHS) reported by Mahmoud *et al.* [9]. Consistent with the reference study, copper was used for the cold plate, water as the coolant, and a constant heat flux of 20,000 W/m^2 was applied to the heating surface. The predicted Nu and ΔP agreed well with the experimental data, with deviations of 2.43–8.29% and 1.94–8.52%, respectively, as summarized in Table 3. Although the benchmark geometry differs from the proposed diamond-baffle cold plate, both systems involve the same fundamental thermo-hydraulic mechanisms, including forced liquid convection through parallel mini-channels and conjugate heat transfer. In addition, the benchmark cases are within the laminar flow regime, which is consistent with most of the configurations investigated in the present study. Therefore, the validation results provide a reasonable basis for applying the adopted numerical methodology and CFD framework to the present thermo-hydraulic analysis.

4. Optimization of Baffle Configurations

4.1. Parametric Investigation

To investigate the influence of diamond-shaped baffles on the thermo-hydraulic performance of the proposed cold plate, a parametric study was conducted under identical operating conditions. The mass flow rate, applied heat flux, and coolant inlet temperature were maintained at 0.06 kg/s, 20,000 W/m^2, and 293 K, respectively, to ensure a consistent comparison among all investigated configurations.

Table 4. Parametric design space and simulation cases

Module	Param.	Range (mm)	Step (mm)	Total
Module 2	d	1;2.41;3.83;5.24;6.66;8.07;9.49	$\sqrt{2}$	70
	h	1–10	1	

The diagonal length (d) and baffle height (h) were selected as the two design variables, while the spacing, number, and arrangement of the baffles were kept constant. The lower bounds of the design variables were selected to avoid configurations in which the baffles were too small for meaningful evaluation of their influence on the thermo-hydraulic performance, whereas the geometric constraints of the cooling channel determined the upper bounds. To maintain geometric similarity and avoid an unnecessary expansion of the design space, the diamond baffle was parameterized by applying a uniform outward offset of 0.5 mm to all four sides at each design level. The corresponding baffle size was then represented by d, resulting in a diagonal increment of $\sqrt{2}$ mm between successive configurations. The investigated parameter ranges and simulation cases are summarized in Table 4.

4.2. Effects of Diamond-Shaped Baffle Geometry

To clarify the influence of the investigated geometric parameters on the overall thermo-hydraulic performance, this section analyzes the effects of d and h on the thermo-hydraulic characteristics, thereby explaining the GRA results and selection of the best-performing configuration under the adopted equal-weight GRA scheme.

Fig. 4 illustrates the effects of the diamond-baffle geometric parameters on Re and ΔP. As shown in Fig. 4(a), Re varies across the investigated d–h design space and is predominantly influenced by h, whereas the influence of d is comparatively limited. Increasing h from 1 to 10 mm generally leads to a decrease in Re, while variations in d produce relatively smaller changes. This behavior results from the combined effects of the effective flow area and hydraulic diameter. Although the reduction in flow area increases the mean coolant velocity, the accompanying change in hydraulic diameter also affects the Reynolds number. Therefore, the observed Re distribution reflects the combined influence of these geometric parameters rather than the effect of either parameter alone.

In contrast, ΔP exhibits a markedly different distribution, as shown in Fig. 4(b). The pressure drop remains relatively low for configurations with small baffle dimensions but increases sharply in the high-blockage region of the design space. The minimum ΔP is 162.06 Pa at d=1 mm and h=1 mm, whereas the maximum reaches 18,621.53 Pa at d=9.49 mm and h=10 mm. These extrema correspond to different d–h combinations and therefore should be interpreted as characteristics of the individual configurations rather than as direct evidence of a causal relationship between the geometric parameters and ΔP. Overall, the increase in ΔP toward the high-blockage region is associated with the combined effects of increased blockage and reduced flow cross-sectional area, which can locally accelerate the coolant, increase viscous friction, and intensify flow separation and recirculation behind the diamond baffles. Consequently, the pressure-drop response needs to be considered together with the thermal responses when identifying a balanced configuration.

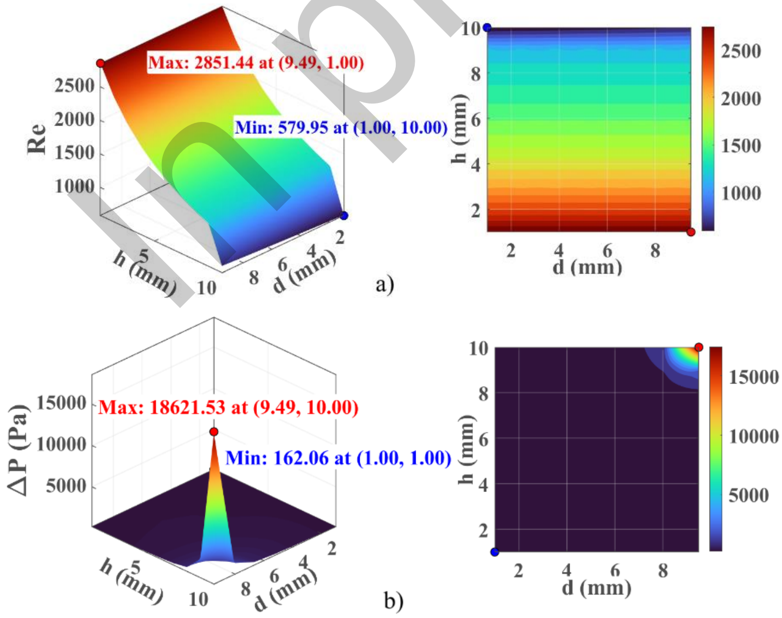

Fig. 4. Effects of geometric parameters on Module 2 performance: (a) The Reynolds number; (b) ΔP

Fig. 5 presents the effects of the diamond-baffle geometric parameters on T_{max} and ΔT. As shown in Fig. 5(a), T_{max} varies nonlinearly across the investigated design space, with the response becoming more favorable as the baffle height increases. The maximum T_{max} of 343.65 K occurs at d = 9.49 mm and h = 1 mm, whereas the minimum value of 304.92 K occurs at d = 9.49 mm and h = 9 mm. These extrema correspond to different configurations and are therefore used to characterize the range of the simulated response rather than to establish a direct causal relationship between d and Tmax. The contour distribution further indicates that the influence of d becomes less pronounced at relatively large values of h. This behavior may be associated with the stronger blockage effect of taller diamond baffles, which can locally accelerate the coolant through the narrowed passages and generate stronger secondary flow and fluid mixing downstream of the baffles. As a result, the thermal boundary layer can be repeatedly disrupted and redeveloped, leading to enhanced convective heat transfer throughout the channel. Although increasing d can also intensify the flow disturbance, its additional contribution becomes less pronounced when the baffle height is sufficiently large, where the mixing enhancement associated with h is already significant.

A similar trend is observed for ΔT, as illustrated in Fig. 5(b). ΔT generally decreases with increasing h, while the influence of d is comparatively smaller. The maximum ΔT of 44.65 K occurs at d=9.49 mm and h=1 mm, whereas the minimum value of 8.83 K is obtained at d = 9.49 mm and h = 8 mm, corresponding to a reduction of approximately 80.2%. The contour distribution indicates that the region of low ΔT expands toward larger baffle heights, suggesting improved temperature uniformity across the cooling surface. This improvement may be associated with intensified coolant mixing and repeated redistribution of the flow field induced by the diamond baffles, which can suppress local hot spots and reduce the temperature difference over the cooling surface. The resulting enhancement is further associated with stronger secondary flow and more effective mixing generated by taller diamond baffles, which promote a more uniform coolant temperature distribution. Overall, within the investigated design space, relatively large values of h, combined with moderate-to-large values of d, are associated with improved thermal performance, although the response depends on the specific d–h combination.

Fig. 5(c) shows the GRG distribution of the investigated configurations. GRG reaches a maximum of 0.868 at d=9.49 mm and h=8 mm, representing the best-performing configuration under the equal-weight GRA scheme, while the minimum value of 0.546 occurs at d=9.49 mm and h=1 mm. GRG generally increases with h up to 8 mm but slightly decreases at 10 mm because the pressure-drop penalty outweighs the additional thermal benefit. Therefore, d=9.49 mm and h=8 mm was selected for the subsequent comparison.

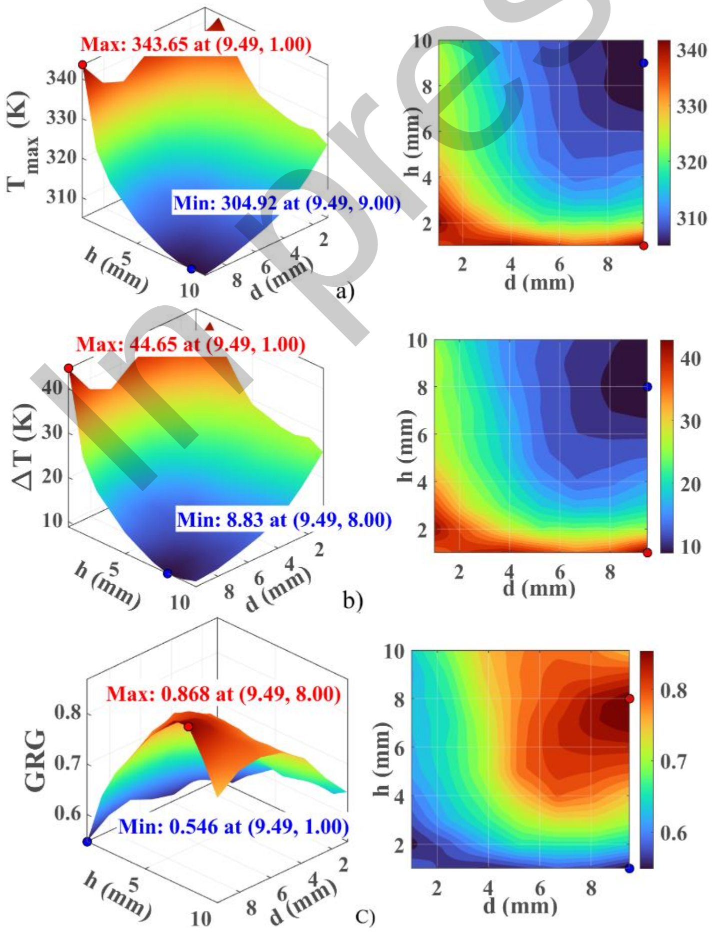

Fig. 5. Effects of geometric parameters on Module 2 performance: (a) $\boldsymbol{T_{max}}$; (b) $\Delta\boldsymbol{T}$; (c) GRG

4.3. Performance Comparison Between the Baseline and Optimized Configurations

Based on the GRA results, the configuration with the highest GRG under the adopted equal-weight scheme was selected as the representative diamond-baffle configuration with d = 9.49 mm, h = 8 mm (Module 2-opt). This section compares its thermo-hydraulic performance with that of the baseline configuration (Module 1) under identical operating conditions to quantify the effectiveness of the proposed enhancement.

Fig. 6 presents the variations of Re and ΔP with mass flow rate for Module 1 and Module 2-opt. As the mass flow rate increases, both Re and ΔP increase monotonically for both configurations. Module 2-opt consistently exhibits a higher Re than Module 1, mainly because the reduced effective flow area increases the coolant velocity, outweighing the opposing effect of the reduced hydraulic diameter. The maximum Re of Module 2-opt is 2193.42, which remains below 2300 and confirms that the flow remains laminar. A more significant difference is observed for ΔP. At 0.02 kg/s, ΔP increases from 22.86 Pa for Module 1 to 111.12 Pa for Module 2-opt, corresponding to an increase of approximately 386%. As the mass flow rate increases to 0.10 kg/s, ΔP further rises from 331.50 Pa to 1704.71 Pa, representing ΔP approximately 5.14 times the baseline value. This substantial increase results from the repeated contraction and expansion of the coolant passage introduced by the diamond baffles, which intensify local flow acceleration, viscous friction, and flow separation. These effects become increasingly pronounced at higher mass flow rates because of the larger coolant momentum, resulting in a nonlinear increase in ΔP. Although Module 2-opt requires a considerably higher pumping power than Module 1, the enhanced flow disturbance generated by the diamond baffles is expected to provide corresponding thermal benefits, which are discussed in the following section.

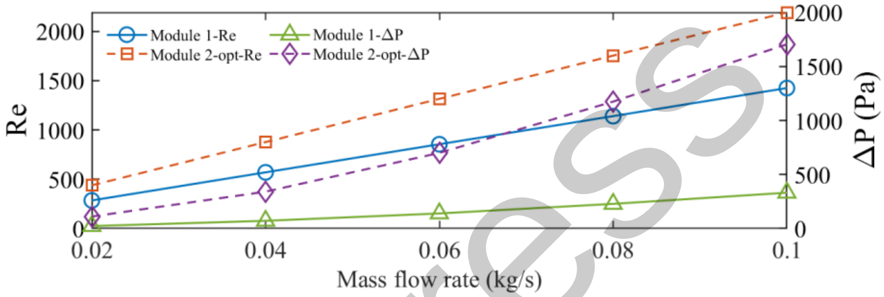

Fig. 6. Comparison of the Re and ΔP between Module 1 and Module 2-opt

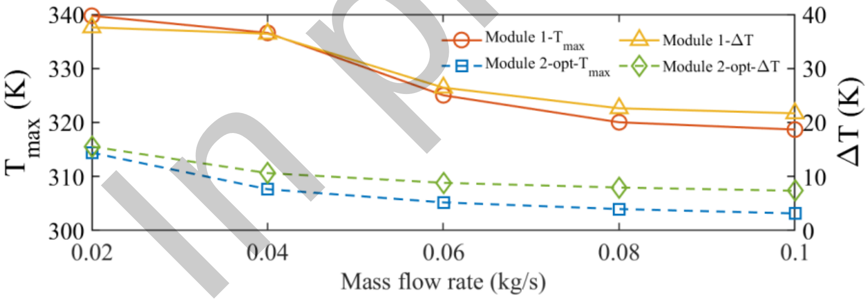

Fig. 7. Comparison of T_{max} and ΔT between Module 1 and Module 2-opt

Fig. 7 compares Tmax and ΔT of Module 1 and Module 2-opt under different mass flow rates. For both configurations, increasing the mass flow rate from 0.02 to 0.10 kg/s continuously reduces both Tmax and ΔT, indicating improved heat removal and temperature uniformity at higher coolant flow rates. Nevertheless, Module 2-opt consistently maintains lower Tmax and ΔT than Module 1 throughout the investigated mass flow rate range. At 0.02 kg/s, Tmax decreases from 339.75 K for Module 1 to 314.39 K for Module 2-opt, corresponding to a reduction of 25.36 K. At the reference operating condition of 0.06 kg/s, Tmax decreases from 325.03 K to 305.20 K, corresponding to a reduction of 19.83 K. At 0.10 kg/s, Tmax is further reduced from 318.69 K to 303.17 K, yielding a reduction of 15.52 K. These results indicate that Module 2-opt provides improved thermal performance over the investigated mass flow rate range.

A similar trend is observed for ΔT. At 0.02 kg/s, ΔT decreases from 37.59 K for Module 1 to 15.54 K for Module 2-opt, corresponding to a reduction of 22.05 K. At the reference operating condition of 0.06 kg/s, ΔT decreases from 26.45 K to 8.83 K, corresponding to a reduction of 17.62 K. As the mass flow rate increases to 0.10 kg/s, ΔT further decreases from 21.69 K to 7.36 K, representing a reduction of 14.33 K. The consistently lower ΔT of Module 2-opt suggests improved temperature uniformity, which may be associated with the repeated disruption of the thermal boundary layer and enhanced coolant mixing induced by the diamond baffles. These effects can promote convective heat transfer and reduce local temperature non-uniformity.

5. Conclusion

This study investigated the thermo-hydraulic characteristics of a parallel-flow cold plate incorporating diamond-shaped baffles using three-dimensional CFD simulations and GRA. The main findings are summarized as follows:

(1) The systematic parametric investigation showed that both d and h affected the thermo-hydraulic performance of the cold plate. Across the investigated design space, Tmax ranged from 343.65 K to 304.92 K, ΔT from 44.65 K to 8.83 K, and ΔP from 162.06 Pa to 18,621.53 Pa. These extrema occurred at different d–h combinations and therefore characterize the response ranges rather than a direct causal relationship with baffle height. These results demonstrate the inherent trade-off between thermal enhancement and hydraulic penalty introduced by the diamond-baffle configuration.

(2) Under the adopted equal-weight GRA scheme, the configuration with d = 9.49 mm and h = 8 mm was identified as the best-performing configuration, achieving the highest GRG of 0.868. Under the reference operating condition (m = 0.06 kg/s), this configuration achieved Tmax = 305.20 K, ΔT = 8.83 K, and ΔP = 699.66 Pa, indicating the most favorable compromise between thermal performance and hydraulic penalty under the adopted weighting scheme.

(3) Compared with Module 1, Module 2-opt consistently exhibited superior thermal performance over the investigated mass flow rate range. At 0.1 kg/s, $T_{\max}$ decreased from 318.69 K to 303.17 K, corresponding to a reduction of 15.52 K (4.87%), while ΔT decreased from 21.69 K to 7.36 K, corresponding to a reduction of 66.07%. This improvement was accompanied by an increase in ΔP from 331.50 Pa to 1704.71 Pa, confirming that the enhanced thermal performance was achieved at the expense of a higher hydraulic penalty. From an engineering perspective, the GRA-based framework provides a flexible approach for selecting suitable cold-plate configurations by adjusting the weighting factors according to the relative importance of thermal and hydraulic performance under specific design requirements.

Although the present CFD model showed good agreement with the reference experimental data, the proposed diamond-baffle design has not yet been experimentally validated, and grid independence was not separately assessed for the complex diamond-baffle and high-flow configurations; both are acknowledged as limitations of the present study. The validation covered the laminar regime, consistent with most investigated cases, whereas a limited number of high-blockage configurations with Re > 2300 may involve transitional effects beyond its scope. Furthermore, only the diagonal length and baffle height were considered, so the identified best-performing design is limited to the investigated design space and the adopted equal-weight GRA scheme. Future work will focus on experimental validation, dedicated grid-convergence assessment for high-blockage and high-flow cases, appropriate flow models for higher-Re conditions, and the effects of additional baffle parameters and arrangements.

Acknowledgments

This research was funded by Hanoi University of Science and Technology (HUST), under project code T2025-PC-037.

References

[1] C. Wu, Y. Sun, H. Tang, S. Zhang, W. Yuan, L. Zhu, and Y. Tang, A review on the liquid cooling thermal management system of lithium-ion batteries, Applied Energy, vol. 375, Dec. 2024, Art. no. 124173. https://doi.org/10.1016/j.apenergy.2024.124173

[2] A. Sharma, M. Khatamifar, W. Lin, and R. Pitchumani, A state-of-the-art review on numerical investigations of liquid-cooled battery thermal management systems for lithium-ion batteries of electric vehicles, Journal of Energy Storage, vol. 101, Nov. 2024, Art. no. 113844. https://doi.org/10.1016/j.est.2024.113844

[3] A. Rahmani, M. Dibaj, and M. Akrami, Recent advancements in battery thermal management systems for enhanced performance of Li-Ion batteries: A comprehensive review, Batteries, vol. 10, iss. 8, p. 265, Jul. 2024. https://doi.org/10.3390/batteries10080265

[4] H. Li, L. Chen, H. Zuo, B. Zhang, and G. Jia, Performance enhancement of a battery thermal management system using novel liquid cold plates with micro-channel featuring pin fins, Energy, vol. 301, Aug. 2024, Art. no. 131731. https://doi.org/10.1016/j.energy.2024.131731

[5] T. Wang, X. Zhang, Q. Zeng, and K. Gao, Thermal management performance of cavity cold plates for pouch Li-ion batteries using in electric vehicles, Energy Science & Engineering, vol. 8, iss. 11, pp. 4082–4093, Nov. 2020. https://doi.org/10.1002/ese3.798

[6] Z. Liu, H. Zhao, Y. Qiu, H. Zeng, and X. Dong, Numerical analysis of topology-optimized cold plates for thermal management of battery packs, Applied Thermal Engineering, vol. 238, Feb. 2024, Art. no. 121983. https://doi.org/10.1016/j.applthermaleng.2023.121983

[7] T. D. Nguyen, D. Nguyen, T. D. Do, D. H. Vu, Y.-H. Chang, and B. V. Le, Thermo-hydraulic optimization of parallel-channel cold plates using CFD: A comparative study of cylindrical and fin-type baffles for battery thermal management, Batteries, vol. 12, iss. 5, p. 183, May 2026. https://doi.org/10.3390/batteries12050183

[8] M. Kılıç, S. Gamsız, and Z. N. Alınca, Comparative evaluation and multi-objective optimization of cold plate designed for the Lithium-ion battery pack of an electrical pickup by using Taguchi–grey relational analysis, Sustainability, vol. 15, iss. 16, Aug. 2023, Art. no. 12391. https://doi.org/10.3390/su151612391

[9] N. S. Mahmoud, H. M. Jaffal, and A. A. Imran, Performance evaluation of serpentine and multi-channel heat sinks based on energy and exergy analyses, Applied Thermal Engineering, vol. 186, Mar. 2021, Art. no. 116475. https://doi.org/10.1016/j.applthermaleng.2020.116475